Available online at www.sciencedirect.com
ScienceDirect
Polymer 48 (2007) 1632–1640
polymer
www.elsevier.com/locate/polymer

Evaluation of amine functionalized polypropylenes as compatibilizers for polypropylene nanocomposites

Lili Cui, D.R. Paul*

Department of Chemical Engineering and Texas Materials Institute, The University of Texas at Austin, Austin, TX 78712-1062, USA

Received 7 November 2006; received in revised form 18 January 2007; accepted 19 January 2007
Available online 25 January 2007

Abstract

The compatibilization effects provided by amine functionalized polypropylenes versus those of a maleated polypropylene, PP-g-MA, for forming polypropylene-based nanocomposites were compared. Amine functionalized polypropylenes were prepared by reaction of maleated polypropylene, PP-g-MA, with 1,12-diaminododecane in the melt to form PP-g-NH_2 which was subsequently protonated to form PP-g-NH_3^+. Nanocomposites were prepared by melt processing using a DSM microcompounder (residence time of 10 min) by blending polypropylene and these functionalized materials with sodium montmorillonite, Na-MMT, and with an organoclay. X-ray and transmission electron microscopy plus tensile modulus tests were used to characterize those nanocomposites. Composites based on Na-MMT as the filler showed almost no improvement of tensile modulus compared to the polymer matrix using any of these functionalized polypropylenes, which indicated that almost no exfoliation was achieved. All the compatibilized nanocomposites using an organoclay, based on quaternary ammonium surfactant modified MMT, as the filler had better clay exfoliation compared to the uncompatibilized PP nanocomposites. Binary and ternary nanocomposites using amine functionalized polypropylenes had good clay exfoliation, but no advantage over those using PP-g-MA. The PP-g-MA/organoclay and PP/PP-g-MA/organoclay nanocomposites showed the most substantial improvements in terms of both mechanical properties and clay exfoliation.

Keywords: Polypropylene; Nanocomposites; Compatibilizer

1. Introduction

Nanocomposites formed from organoclays represent a potentially attractive approach for improving some performance characteristics (mechanical, thermal, barrier, etc) of polymers without a significant increase in material mass because the high aspect ratio of the clay platelets permits significant reinforcement at low loadings. However, the key challenge to realizing this potential is to achieve a high degree of exfoliation of the aluminosilicate layers within the polymer matrix using a convenient and economical process, like melt compounding. Extensive studies have been reported recently on the effects of processing variables, organoclay structure, organoclay–polymer interaction, etc on exfoliation and property development [1–5]. From this background, it has become clear that unmodified polyolefins lack the intrinsic thermodynamic affinity with the currently available organoclays to form well-exfoliated nanocomposites [1,2,6,7]; yet, in principle, materials like polypropylene, PP, would offer the greatest commercial opportunity for such technology. The use of a ''compatibilizing'' component has proved to be at least a partial solution to this problem; maleated polypropylene, PP-g-MA, has become the widely accepted standard for this function [8–12]. Even though PP-based nanocomposites containing PP-g-MA are not as well exfoliated as those based on more polar polymers like nylon 6 [4,5,13], this approach has allowed commercialization to go forward.

Clearly more extensive utilization of PP-based nanocomposites would be possible if a more effective or less expensive compatibilizer was available. The purpose of this study is to

* Corresponding author. Tel.: +1 512 471 5392; fax: +1 512 471 0542.
E-mail address: drp@che.utexas.edu (D.R. Paul).

0032-3861/$ - see front matter © 2007 Elsevier Ltd. All rights reserved.
doi:10.1016/j.polymer.2007.01.036

explore the possibility of other functional PPs that might serve as a better compatibilizer than PP-g-MA. It has been reported [14] that an ammonium terminated PP (PP-t-NH_3^+) forms a very well-exfoliated nanocomposite when combined with clay using a static melt intercalation technique; this chemical approach seems promising. Inspired by this idea, we explore here a practical way to produce amine funtionalized PP materials and test their effectiveness as compatibilizers for PP nanocomposites using conventional melt processing techniques. Wang et al. [14] also proposed a possible cation exchange reaction between PP-t-NH_3^+ and the sodium cations at the MMT surfaces during the formation of nanocomposites, which would exfoliate the clay platelets. To test this idea, we used both sodium montmorillonite and an ammonium surfactant modified montmorillonite organoclay as the nanofillers for the nanocomposites.

2. Experimental

2.1. Materials

The materials used in this study are described in Table 1. The PP matrix polymer is of commercial injection molding grade from Basell with a melt index of 37.

The PP-g-MA selected for this work was PB3200, supplied by Crompton, which contains 1 wt% maleic anhydride groups; this material has been shown by other studies to be effective for promoting exfoliation of organoclays in polypropylene nanocomposites [15–19]. It has a high melt index because of the chain scission that accompanies grafting. Such materials are made by reactive extrusion of PP with maleic anhydride and a peroxide [20,21]. The free radicals produced by the peroxide abstract hydrogens from the carbon backbone of PP. These sites allow grafting of maleic anhydride, typically only one unit is added at each site; however, the hydrogen abstraction also leads to chain scission of the PP backbone at this point. Thus, there is a tendency for the maleic anhydride units to exist at the end of the broken PP chain; such chains would approximate an end functionalized polypropylene, i.e., PP-t-MA. Of course, this is an over simplification of the structure of PP-g-MA, and some chains may contain more MA units than the single one envisioned by the above scenario; thus, some PP-g-MA may be multifunctional. The amine functionalized compatibilizer was prepared from this PP-g-MA in our laboratory by procedures explained later.

Sodium montmorillonite and an organoclay (Cloisite 20A) based on dimethyl, dihydrogenated tallow quaternary ammonium, $M_2(HT)_2$, were provided by Southern Clay Products Inc. The exchange ratio of the organic ammonium ion on MMT was 95 meq/100 g clay (MER). The organic loading was determined by the mass loss on ignition (LOI) to be 38 wt%. These two clays were selected for the following reasons. Wang et al. [14] speculated that the cations of the protonated amine grafted to PP might exchange with the sodium ions of Na-MMT which would separate the clay platelets from each other and facilitate exfoliation. Recent studies have shown that for each polymer matrix there is an optimum structure of the surfactant on the organoclay for achieving exfoliation or dispersion [22,23]; Cloisite 20A has been shown to be a good choice for polyolefins, which was the basis for including it in this study.

2.2. Preparation of nanocomposites

All the nanocomposites were prepared using a DSM Micro 5 melt compounder, which has a net barrel capacity of 5 cm^3, using a screw speed of 100 rpm and a barrel temperature of 190 °C, with all the components added at the same time. All the materials were dried in a vacuum oven at 80 °C overnight prior to use.

Test bars were formed using a DSM micro-injection molding machine with the barrel temperature set at 195 °C and the mold temperature at 35 °C. The dimensions of the molded specimen were $0.32 \times 1.00 \times 7.10$ cm^3. The injection molding pressure and holding pressure were both set at 40 bar. The data below are reported in terms of the weight percent montmorillonite (MMT) in the composites rather than the amount of organoclay, since the silicate is the reinforcing component.

2.3. Characterization

Mechanical property tests were performed on an Instron model 1137 upgraded for computerized data acquisition. Modulus values were determined using an extensometer at a crosshead speed of 0.51 cm/min. Because dumb-bell shaped specimens could not be prepared by the available molds for the micro-injection molding machine, failure properties were not measured.

X-ray diffraction scans were obtained using a Scintag XDS 2000 diffractometer in the reflection mode, with an incident X-ray wavelength of 1.541 Å at a scan rate of 1.0 deg/min

Table 1
Materials used in this study

Materials	Commercial designation	Supplier	Properties
Polypropylene	Pro-Fax PH020	Basell	MI = 37; density = 0.902 g/cm^3
PP-g-MA	PB3200	Crompton	MI = 105; density = 0.91 g/cm^3; MA content = 1.0 wt%; $\overline{M}_w$ = 90,000, MWD ≈ 2.7
Sodium MMT (Na-MMT)	Cloisite NA+	Southern Clay Product	Percent loss on ignition = 7; d_{001} = 1.17 nm
Organoclay	Cloisite 20A	Southern Clay Product	Surfactant: Dimethyl, dihydrogenated tallow quaternary ammonium; surfactant concentration = 95 meq/100 g clay; percent loss on ignition = 38; d_{001} = 2.42 nm
Diamine	1,12-Diaminododecane	Sigma–Aldrich	Melting point = 69 °C; boiling point = 304 °C

over the range of $2\theta = 1-12^\circ$. The skin areas of the injection molded rectangular bars were scanned while the clay was analyzed in powder form.

TEM images were obtained using a JEOL 2010F transmission electron microscope operating under an accelerating voltage of 120 kV. Ultra-thin sections (~50 nm) were cut from the central part of the injection molded bars parallel to the flow direction under cryogenic conditions using a RMC PowerTome XL microtome.

3. Preparation of amine functionalized polypropylene (PP-g-NH_2 and PP-g-NH_3^+)

3.1. Reactive blending

The amine functionalized polypropylene was prepared by reactive blending of PP-g-MA with 1,12-diaminododecane from Aldrich. Two factors guided the choice of this diamine. The reactions of aliphatic amines with anhydrides have been reported [24] to be faster than aromatic amines and can lead to higher reaction extents. A diamine with high molecular weight, which tends to have high melting and boiling points, is a requirement for the current melt reactive blending technique at high temperatures to prevent diamine loss by evaporation.

Approximately 45 g of PP-g-MA was first introduced into the mixing chamber of a Brabender mixer at 195 °C and 50 rpm. After PP-g-MA was melted and the torque stabilized, 1,12-diaminododecane was added in an amount to give a specified molar ratio of amine groups to maleic anhydride groups. After mixing for another 5.5 min, samples were taken from the mixing chamber, solidified and ground to form a powder which was purified by soxhlet extraction, using xylene as the solvent, for 24 h to remove the excess diamine.

Some of the purified PP-g-NH_2 was further treated with acid to form PP-g-NH_3^+. The protonation was done in a reflux of HCl solution in toluene at 70 °C for 7 h under N_2 protection [14].

3.2. Reaction scheme

The reaction between an amine and an anhydride unit, shown in Fig. 1, first leads to an amide and a carboxylic acid or amic acid; this is a very fast reaction and can happen even at room temperature. The subsequent cyclization step is comparatively much slower and is reversible [24] but can be effectively completed at melt processing temperatures.

During the reactive blending, the torque values were recorded. Fig. 2 compares the torque evolution for different reactant ratios (x = the molar ratio of amine groups to maleic anhydride groups). For pure PP-g-MA, the torque stabilizes after 3–4 min. After adding the diamine, the torque increased immediately and dramatically, which means at 195 °C the reactions suggested in Fig. 1 occur very fast. The torque increase is due to the increase in molecular weight and possible crosslinking when one amine of the diamine reacts with one PP-g-MA molecule while the other amine reacts with a different PP-g-MA molecule as suggested in Fig. 1. If each PP-g-MA

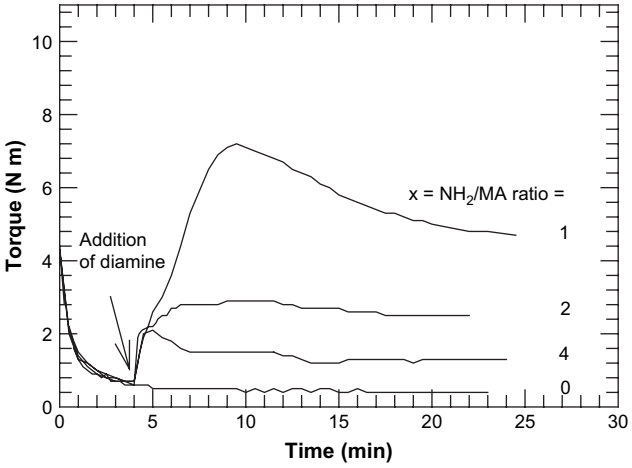

Fig. 2. Brabender torque evolution during reaction of PP-g-MA with diamine.

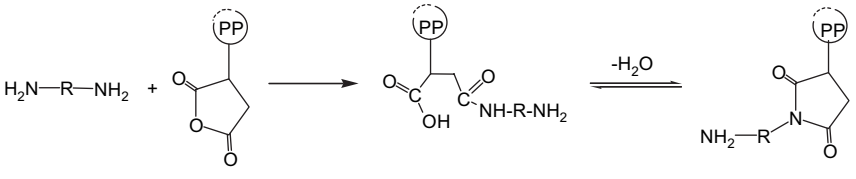

Possible crosslinking:

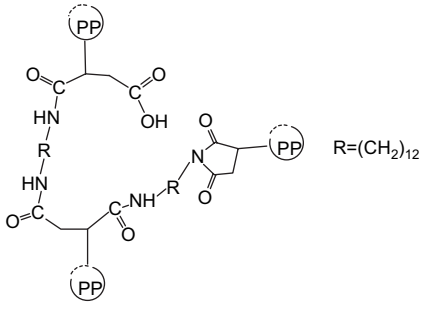

Fig. 1. Reaction of 1,12-diaminododecane with maleic anhydride grafted polypropylene.

molecule contained only one maleic anhydride unit, these reactions with the diamine should lead only to chain extension. However, to the extent that the PP-g-MA material contains molecules with more than one maleic anhydride unit, this reaction can lead to crosslinking [24]. An excess of diamine would tend to reduce the possibility of coupling two PP-g-MA molecules or crosslinking and would favor the desired result of only one of the amines on the diamine reacting with an anhydride leaving the other amine unreacted. The results show that as the value of x increases beyond unity, the maximum value of the torque decreases and the time needed to reach the maximum becomes shorter. This indicates that excess diamine tends to diminish the extent of chain coupling or crosslinking as would be expected. In this study, $x = 4$ was chosen for preparation of the amine functionalized PP, since the extent of chain coupling or crosslinking is minimized. The progressive decrease of the torque after the maximum in this case might be attributed in part to the excess diamine acting as a plasticizer; however, reduced molecular weight build up is likely the dominant effect.

3.3. FTIR characterization of PP-g-NH_2

FTIR was used to characterize the product structure, see Fig. 3 and Table 2 [25,26]. The disappearance of the anhydride carbonyl stretching absorption at 1780 cm^{-1} indicates a considerable extent of reaction. Formation of the imide groups through cyclization of the acid and amide can also be identified by the new absorption band at 1770 cm^{-1}. Imide units have been reported to have carbonyl absorption at 1770 cm^{-1} (asymmetrical stretching) and 1700–1720 cm^{-1} (symmetrical stretching) [25,26]. The absorption due to symmetrical carbonyl stretching of imide groups superimposed on the strong absorption at 1710 cm^{-1} due to carbonyl stretching of the carboxylic acid.

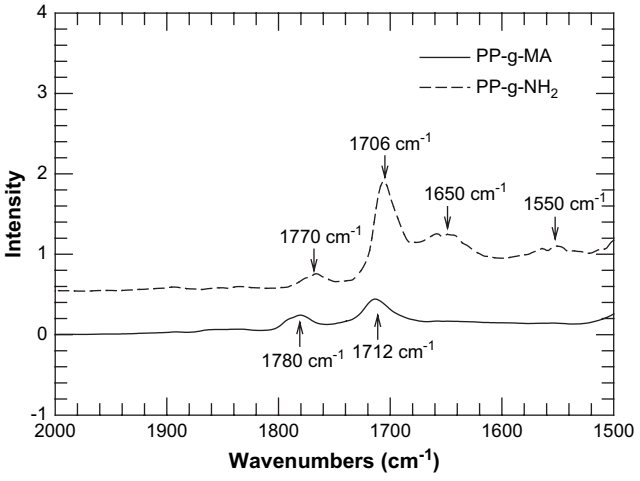

Fig. 3. FTIR spectra of PP-g-MA and PP-g-NH_2.

Table 2
Infrared peak assignments

Peak location (cm^{-1})	Group assignment
1550	Secondary amide groups
1650	Secondary amide groups
1706	Carboxylic acid carbonyl stretching
1712	Imide carbonyl symmetrical stretching
1770	Imide carbonyl asymmetrical stretching
1780	Anhydride carbonyl stretching

4. Results

4.1. Force recordings via DSM microcompounder

The force measurement capability of the DSM microcompounder provides similar rheological information as the torque measurement does in the Brabender mixer. Thus, force evolution versus time traces on the DSM microcompounder were recorded and are shown in Fig. 4 for virgin PP, PP-g-MA, and PP-g-NH_2. The force for PP-g-NH_2 is about three times higher than that for PP-g-MA while PP falls in between. This observation is consistent with the equilibrium torque recordings from the Brabender during the reaction used to make the amine functionalized PP. This suggests that even at the amine to anhydride ratio of 4 used to make the PP-g-NH_2, some chain coupling or crosslinking still occurs. Note that owing to the purification scheme used, no free diamine should be present in these materials during processing in the DSM microcompounder.

4.2. Mechanical properties

The moduli of binary nanocomposites formed from neat polypropylene and the various functionalized polypropylenes and sodium montmorillonite or $M_2(HT)_2$ organoclay are compared in Table 3. The absolute moduli for the neat polymers and their composites containing ~5 wt% MMT are listed along with the ratio of the composite modulus to that of the matrix which indicates the extent of reinforcement by the nanofiller and is a rough indicator of the extent of exfoliation.

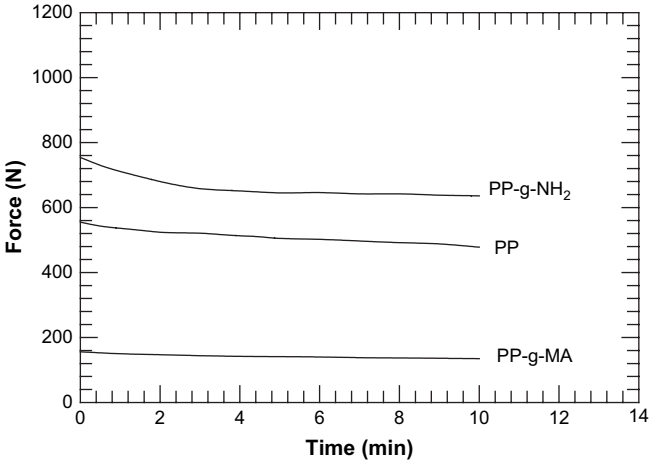

Fig. 4. Force versus time relationships during DSM compounding.

Table 3
Modulus comparisons for two component nanocomposites

Matrix polymer	Filler	Modulus of pure polymer (GPa)		Modulus of nanocomposites with 5 wt% MMT (GPa)		Modulus ratio of nanocomposite to polymer matrix
			Std. Dev		Std. Dev	
PP	Na-MMT	1.58	0.047	1.57	0.021	0.99
PP-g-NH_2	Na-MMT	1.72	0.028	1.90	0.021	1.10
PP-g-NH_3^+	Na-MMT	1.80	0.042	1.74	0.127	0.97
PP-g-MA	Na-MMT	1.49	0.035	1.49	0.042	1.00
PP	Cloisite 20A	1.58	0.047	1.74	0.036	1.10
PP-g-NH_2	Cloisite 20A	1.72	0.028	1.91	0.049	1.11
PP-g-NH_3^+	Cloisite 20A	1.80	0.042	2.34	0.078	1.30
PP-g-MA	Cloisite 20A	1.49	0.035	2.14	0.165	1.44

When using sodium MMT as the filler, the improvements in modulus are quite small for each composite; whereas, when the organoclay, Cloisite 20A, is the nanofiller, all the composites show greater improvements in modulus. However, PP-g-MA nanocomposites show the most substantial improvement, while the composites based on unmodified PP have the least improvement. The composites based on PP-g-NH_3^+ and PP-g-NH_2 fall in between.

Ternary nanocomposites based on PP/functionalized PP/clay were prepared at several MMT loadings to obtain a more complete picture of the relative benefit of each functionalized PP as a compatibilizer for nanocomposites formed by melt processing. The ratio of functionalized PP to clay was set at 1; this ratio has been shown by several studies in our laboratory [15–17] to be an optimum level of PP-g-MA for compatibilization of PP/organoclay mixtures. Higher ratios lead to very little additional benefit. Since PP-g-MA is relatively expensive compared to PP, there is an incentive to use no more than necessary to achieve effective dispersion of the organoclay or property improvement.

For the composites using sodium MMT as the filler, Fig. 5 shows almost no modulus improvement at any loading. Apparently, the dispersion of the sodium MMT is very poor with almost no exfoliation achieved; slight property improvements could only be realized at high filler loadings as in composites with conventional fillers [15].

Fig. 6 shows the effect of montmorillonite content on the modulus for four different systems based on the organoclay Cloisite 20A. The addition of organoclay to the polymer matrix produces significant increases in the modulus in all cases. Each system containing a compatibilizer shows a higher modulus increase than the uncompatibilized system, and this difference becomes larger with increasing MMT loading. Among the three compatibilized systems, those based on PP-g-MA show the highest modulus, the one based on PP-g-NH_3^+ show the second highest modulus improvement, while those based on PP-g-NH_2 rank third. These results agree with the TEM and WAXS observations discussed below.

4.3. Wide angle X-ray scattering

The morphology of the composites determined by WAXS and TEM described in this and the next section complement the property determinations discussed earlier. Fig. 7 compares the WAXS scans for pure sodium montmorillonite and binary composites containing ~5 wt% MMT. The scan for the pure Na-MMT reveals an intense peak around $2\theta = 7.3°$, which indicates the basal spacing of the as received Na-MMT ($d_{001} = 1.21$ nm). All the composites showed corresponding peaks, but these peaks are largely shifted to higher angles ($d_{001} = 0.98$ nm). This shifting is probably due to the loss of water in clay galleries during the melt processing; dry Na-MMT has a basal spacing of 0.96 nm [27,28], which is close to the values shown by the composites formed here. In Fig. 8, similar behavior is seen for ternary composites based on Na-MMT.

Fig. 9 compares the WAXS scans for pure Cloisite 20A organoclay and binary nanocomposites containing ~5 wt% MMT. The scan for the pure organoclay reveals an intense

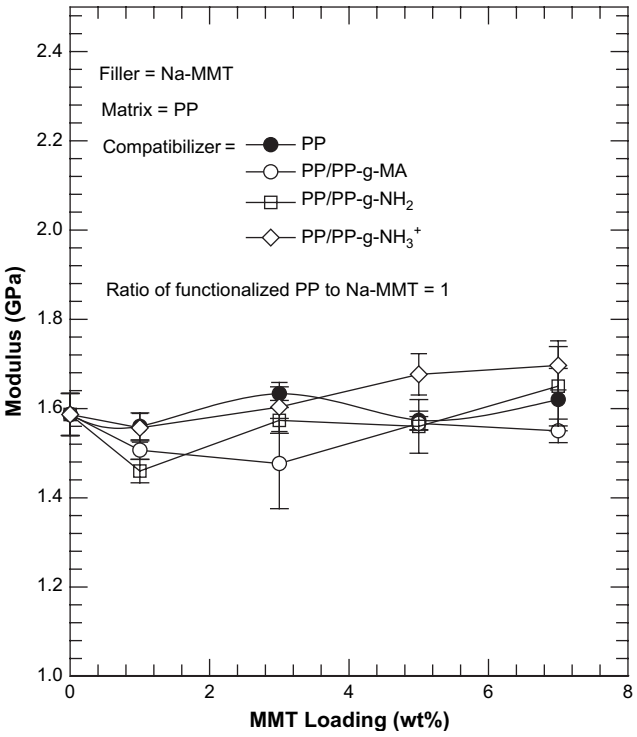

Fig. 5. Effect of MMT content on the tensile modulus of PP/Na-MMT and PP/functionalized PP/Na-MMT (ratio of functionalized PP to clay = 1) composites.

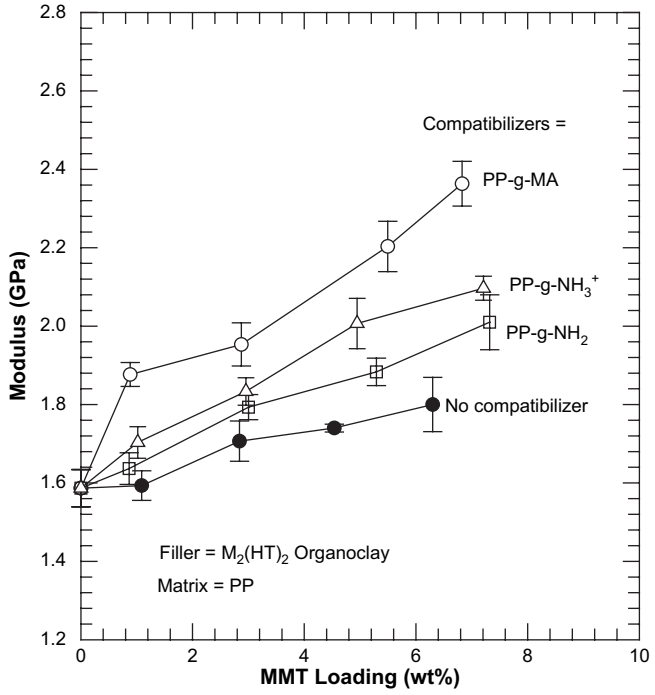

Fig. 6. Effect of MMT content on the tensile modulus of PP/functionalized PP/organoclay (ratio of functionalized PP to organoclay = 1) nanocomposites.

peak around $2\theta = 3.6^\circ$, which is characteristic of the basal spacing of the modified layered silicate; nanocomposites, except for unmodified PP, do not show a distinctive basal reflection which is consistent with a more well dispersed or exfoliated structure. However, there are slight hints of curvature that could be interpreted as an extremely broad peak suggesting these three systems could be almost but not completely exfoliated; this extremely broad peak is shifted largely to lower angles suggesting some intercalation into the organoclay galleries [7,29].

Fig. 10 shows the WAXS scans of pure organoclay and ternary PP/functionalized PP/organoclay nanocomposites with 5 wt% MMT. The ratio of functionalized PP to organoclay

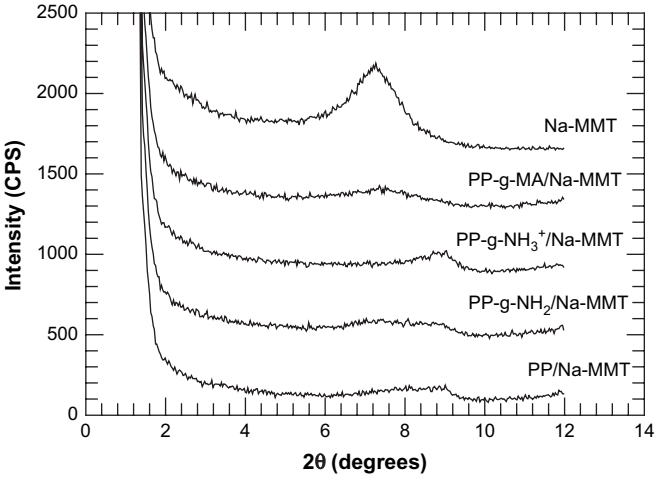

Fig. 7. X-ray scans for pure Na-MMT and polymer/Na-MMT nanocomposites containing ~5 wt% MMT. The curves are vertically offset for clarity.

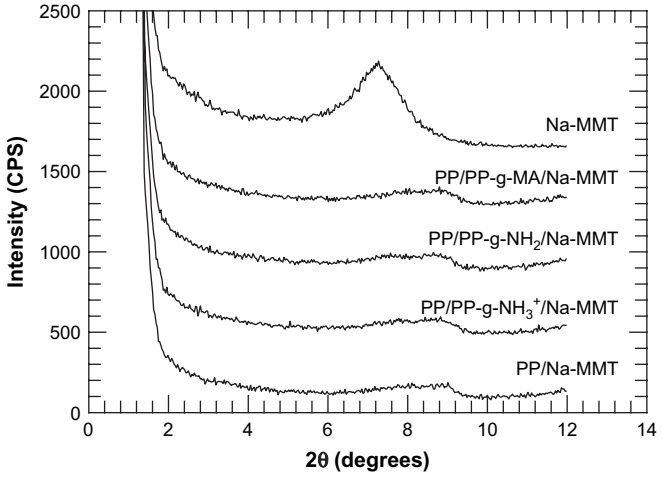

Fig. 8. X-ray scans for pure Na-MMT, PP/Na-MMT, and PP/functionalized PP/Na-MMT nanocomposites containing ~5 wt% MMT. The curves are vertically offset for clarity.

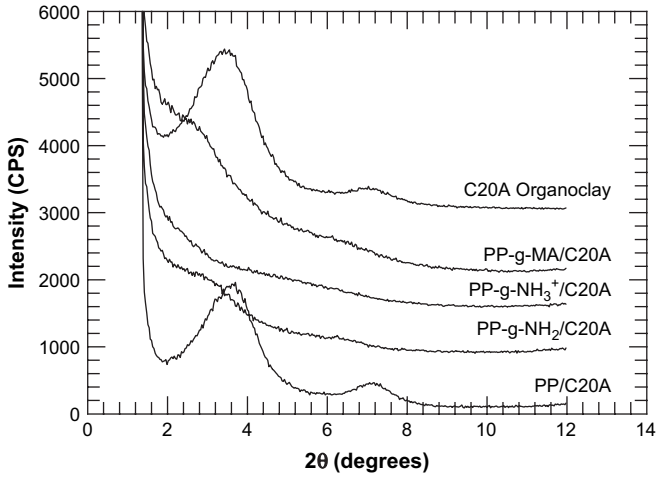

Fig. 9. X-ray scans for pure C20A organoclay and polymer/organoclay nanocomposites containing ~5 wt% MMT. The curves are vertically offset for clarity.

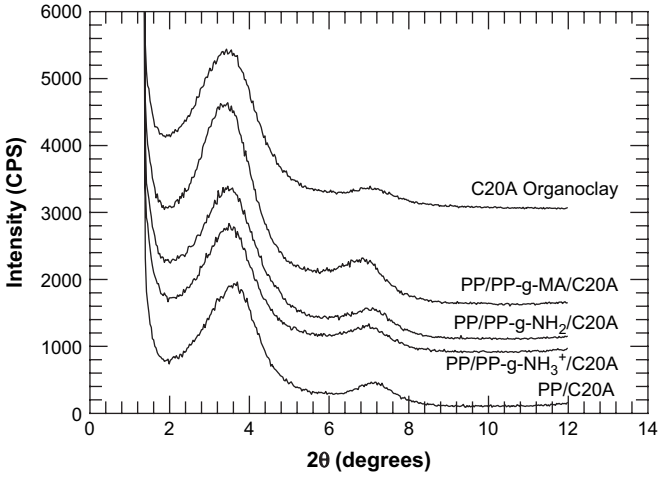

Fig. 10. X-ray scans for pure C20A organoclay, PP/C20A, and PP/functionalized PP/organoclay nanocomposites containing ~5 wt% MMT. The curves are vertically offset for clarity.

used was set at 1. The nanocomposites show very similar distinctive peaks as the pure organoclay indicative of the presence of clay tactoids in these composites [7,29]. These results agree well with the morphologies seen by TEM.

4.4. Transmission electron microscopy

Fig. 11 shows TEM images of nanocomposites formed from the different polymer matrices and the organoclay, i.e., PP/organoclay, PP-g-MA/organoclay, PP-g-NH_2/organoclay and PP-g-NH_3^+/organoclay; the MMT loadings in all cases are ~5 wt%. The PP/organoclay composite contains many large aggregates of micro-sized particles, which means the non-polar polypropylene matrix does not exfoliate the organoclay. The PP-g-MA/organoclay nanocomposite shows much better exfoliation of the organoclay; most of the particles are individual platelets. The nanocomposites formed from PP-g-NH_2 and PP-g-NH_3^+ also have very small particles indicating good, but not complete, exfoliation of the organoclay.

Fig. 12 shows the morphology of the nanocomposites formed from ternary nanocomposites based on PP, organoclay, and the functionalized PPs, acting as the compatibilizer at MMT loadings of ~5 wt%. The ratio of functionalized PP to organoclay was set at 1. Comparing these images for the three compatibilized nanocomposites, it is apparent that the one based on PP-g-MA gives the best exfoliation of the organoclay, while the other two nanocomposites based on amine functionalized PP do not show good exfoliation. Protonation seems to improve the exfoliation; the nanocomposite based on PP-g-NH_3^+ has somewhat better organoclay exfoliation

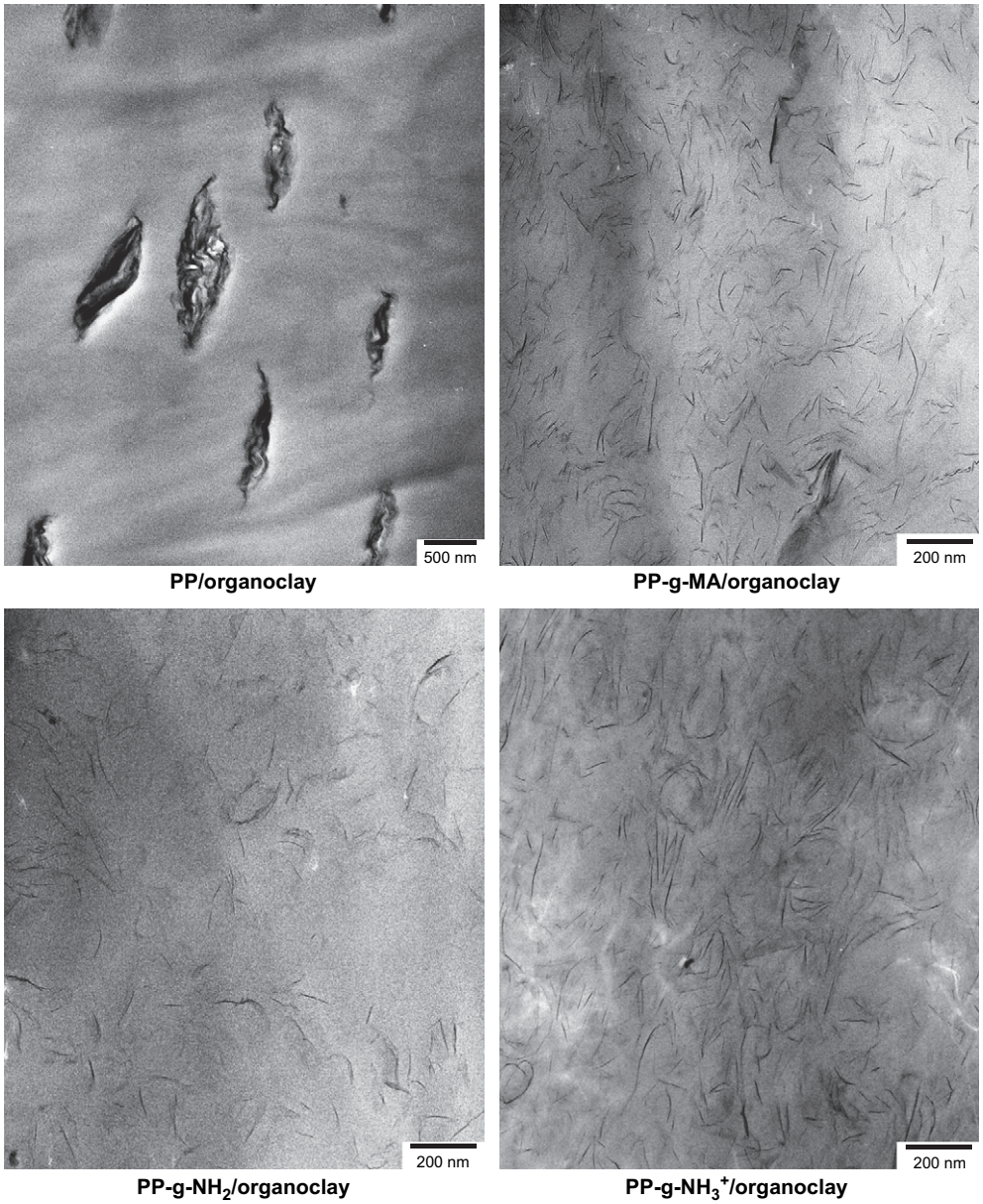

Fig. 11. TEM micrographs for PP and functionalized PP/organoclay nanocomposites containing ~5 wt% MMT. Images were taken from the core of injection molded specimens and viewed perpendicular to the flow direction within the molded bars.

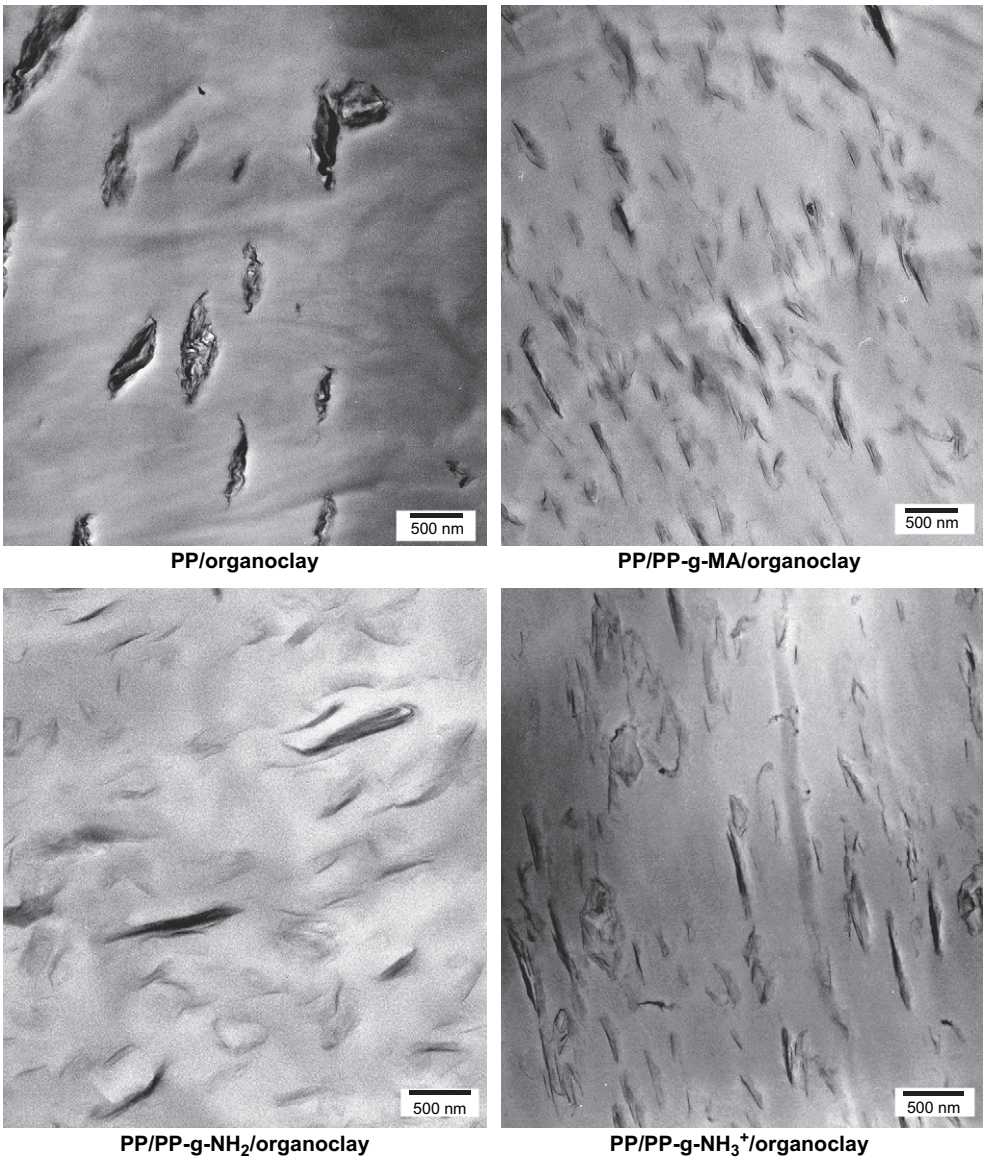

Fig. 12. TEM micrographs of PP/organoclay and PP/functionalized PP/organoclay nanocomposites containing ~5 wt% MMT and a functionalized PP/organoclay ratio of 1. Images were taken from the core of injection molded specimens and viewed perpendicular to the flow direction within the molded bars.

than the one based on PP-g-NH_2, which is consistent with the modulus results.

5. Discussion

Maleic anhydride grafted polypropylenes, PP-g-MA, typically have one anhydride unit located at the chain end owing to the chain scission that accompanies grafting. A simple scheme was used here to form amine terminated polypropylene analogous to similar materials, PP-t-NH_2 and PP-t-NH_3^+, described previously using a different approach [14]. Wang et al. [14] claimed that a molten mixture of PP-t-NH_3^+ with Na-MMT held in a static condition for 2 h led to a high level of exfoliation perhaps due to an ion exchange mechanism. The purpose of the current work is to determine if this concept can be implemented in a practical melt processing scheme to make high performance polypropylene-based nanocomposites.

Thus, preparation of nanocomposites from both Na-MMT and an organoclay, Cloisite 20A, using our amine functionalized polypropylenes, PP-g-NH_2 and PP-g-NH_3^+, as the matrix and as a compatibilizer with polypropylene was explored using a melt compounding approach. Very little exfoliation was achieved with Na-MMT while better exfoliation was observed with the organoclay. PP-g-NH_3^+ led to better exfoliation than PP-g-NH_2; however, neither amine functionalized polypropylene is superior to PP-g-MA as a matrix nor as a compatibilizer for formation of polypropylene-based nanocomposites.

Clearly, kinetic factors may explain the differences between the observations reported here versus the claims by Wang et al. [14]. In their static melt process, the polymer and clay mixture were heated at 190 °C for 2 h, while under the current melt processing conditions, the mixture only stays in the DSM microcompounder for 10 min, which is a longer time than typical

for conventional melt processing but may not be enough time for the proposed ion exchange to happen. Another possible factor may be that the molecular structures and molecular weights of the PP-g-NH_2 and PP-g-NH_3^+ formed via the diamine/anhydride reaction scheme used here are different from that synthesized by Wang et al. Detailed structural information would need to be developed to assess their possibility.

6. Conclusion

Wang et al. [14] described a method to synthesize amine functionalized polypropylene by a polymerization route and suggested that these materials lead to exfoliated nanocomposites via a long time static melt intercalation step. We report here an alternate scheme to produce amine functionalized polypropylene using reactive melt blending. The latter amine functionalized polypropylenes were melt mixed with sodium montmorillonite and an organoclay to see if this provides an industrially viable approach to form well-exfoliated nanocomposites. Mechanical properties and transmission electron microscopy results show that the amine functionalized polypropylenes and the melt mixing methods described here do not provide a practical route for forming highly exfoliated polypropylene nanocomposites. It appears that the polar $-NH_2$ group or the ionic $-NH_3^+$ group apparently do not provide a better interaction for exfoliation of the organoclay than does the anhydride units of the starting PP-g-MA material.

Acknowledgement

The authors thank D.L. Hunter of Southern Clay Products, Inc. for many helpful discussions and for providing materials and other assistance.

References

[1] Wang Y, Chen FB, Wu KC, Wang JC. Polymer Engineering and Science 2006;46(3):289–302.
[2] Modesti M, Lorenzetti A, Bon D, Besco S. Polymer 2005;46(23): 10237–45.
[3] Shah RK, Paul DR. PMSE Preprints 2004;91982–3.
[4] Fornes TD, Hunter DL, Paul DR. Macromolecules 2004;37(5):1793–8.
[5] Shah RK, Paul DR. Polymer 2004;45(9):2991–3000.
[6] Ellis TS, D'Angelo JS. Journal of Applied Polymer Science 2003;90(6):1639–47.
[7] Shah RK, Paul DR. Polymer 2006;47(11):4075–84.
[8] Varela C, Rosales C, Perera R, Matos M, Poirier T, Blunda J, et al. Polymer Composites 2006;27(4):451–60.
[9] Lopez-Quintanilla ML, Sanchez-Valdes S, Ramos de Valle LF, Guedea Miranda R. Polymer Bulletin (Heidelberg, Germany) 2006;57(3): 385–93.
[10] Galgali G, Ramesh C, Lele A. Macromolecules 2001;34(4):852–8.
[11] Maiti P, Nam PH, Okamoto M, Hasegawa N, Usuki A. Macromolecules 2002;35(6):2042–9.
[12] Reichert P, Nitz H, Klinke S, Brandsch R, Thomann R, Mulhaupt R. Macromolecular Materials and Engineering 2000;275:8–17.
[13] Chavarria F, Paul DR. Polymer 2004;45(25):8501–15.
[14] Wang ZM, Nakajima H, Manias E, Chung TC. Macromolecules 2003;36(24):8919–22.
[15] Lee H-s, Fasulo PD, Rodgers WR, Paul DR. Polymer 2005;46(25): 11673–89.
[16] Lee H-s, Fasulo PD, Rodgers WR, Paul DR. Polymer 2006;47(10): 3528–39.
[17] Kim DH, Fasulo PD, Rodgers WR, Paul DR. 64th Annual Technical Conference – Society of Plastics Engineers; 2006. p. 592–6.
[18] Wang Y, Chen F-B, Wu K-C. Journal of Applied Polymer Science 2004;93(1):100–12.
[19] Wang Y, Chen F-B, Li Y-C, Wu K-C. Composites, Part B: Engineering 2004;35(2):111–24.
[20] De Roover B, Sclavons M, Carlier V, Devaux J, Legras R, Momtaz A. Journal of Polymer Science, Part A: Polymer Chemistry 1995;33(5): 829–42.
[21] Shi D, Yang J, Yao Z, Wang Y, Huang H, Jing W, et al. Polymer 2001;42(13):5549–57.
[22] Shah RK, Krishnaswamy RK, Paul DR. 64th Annual Technical Conference – Society of Plastics Engineers. 2006. p. 597–601.
[23] Paul DR. Abstracts of Papers. 229th ACS National Meeting, San Diego, CA, United States. March 13–17; 2005, 2005POLY-205.
[24] Colbeaux A, Fenouillot F, Gerard J-F, Taha M, Wautier H. Polymer International 2005;54(4):692–7.
[25] Scott C, Macosko C. Journal of Polymer Science, Part B: Polymer Physics 1994;32(2):205–13.
[26] Song Z, Baker WE. Journal of Polymer Science, Part A: Polymer Chemistry 1992;30(8):1589–600.
[27] Hv Olphen. An introduction to clay colloid chemistry. New York: Wiley; 1966.
[28] Paul DR, Zeng QH, Yu AB, Lu GQ. Journal of Colloid and Interface Science 2005;292(2):462–8.
[29] Hotta S, Paul DR. Polymer 2004;45(22):7639–54.